

Age Hardenable Nickel-Based Alloy Developments and Research for New High Temperature Power Cycles



John P. Shingledecker and John A. Siefert

Abstract Advanced Ultrasupercritical (A-USC) steam Rankine cycles and Supercritical Carbon Dioxide (sCO₂) Brayton cycles are under intensive development to enable low carbon generation of electricity. These high-efficiency power cycles, aimed at fossil and in some cases renewable energy, require higher temperatures and pressures compared to traditional steam cycles for pressuring retaining components such as tubing, piping, heat exchangers, and turbine casings. Extensive research and development to produce and characterize age-hardenable nickel-based alloys containing Al, Ti, and Nb in judicious amounts have allowed designers to now consider supercritical fluid temperatures up to ~760 °C which is much greater than today's supercritical steam technology based on steel metallurgy up to ~610 °C. This paper will focus on the alloys developed around the world to enable these advanced power cycles, and a discussion on their key properties: long-term creep strength (100,000 h+), fabricability, and weldability/weld performance. Most of these alloys contain less than 25% gamma prime, such as alloy 740H, 263, and 282, due to the need for heavy section weldability, unique to these applications. While welding processes have now been developed for many of these alloys using a variety of filler metals and processes, key research questions remain on the applicability of processes to field power plant erection, the potential for cracking to occur during service, and the long-term weld creep and creep-fatigue performance.

Keywords Steam boilers • Steam turbines • Inconel[®] alloy[®] 740H Welding

J. P. Shingledecker (✉) · J. A. Siefert
Electric Power Research Institute, Charlotte, NC, USA
e-mail: jshingledecker@epri.com

J. A. Siefert
e-mail: jsiefert@epri.com

© The Minerals, Metals & Materials Society 2018
E. Ott et al. (Eds.), *Proceedings of the 9th International Symposium on Superalloy 718 & Derivatives: Energy, Aerospace, and Industrial Applications*, The Minerals, Metals & Materials Series, https://doi.org/10.1007/978-3-319-89480-5_1

Introduction to Advanced Energy Systems Requiring Nickel-Based Alloys

National and Global Trends

In 2015, the electricity produced from coal and natural gas in the U.S. was approximately equal at 34% each, representing 68% of the total electricity generated with the remaining major sources being nuclear at 20% and all renewables (hydro, wind, solar, biomass, etc.) at 12%. In 2016, for the first time in the history of the U. S., electricity produced from natural gas exceeded that of coal generation 36 to 31% as shown in Fig. 1 [1]. Globally coal and natural gas continue to be the predominate fuels for the production of energy [2]. While future projection for the exact mix of fossil fuels remain uncertain both nationally and globally, the world is projected to need more electricity with fossil fuels being a major source of new generation [3]. In the US, the need for electricity continues to increase. As illustrated in Fig. 2, which shows the historical use of electricity as a percentage of the total energy use in the U.S., efficient electrification for residential, commercial, and industrial sectors has steadily increased for over 50 years as electrification is recognized as a key element of the future energy in the U.S. [4]. The need for environmentally responsible electricity through significant reductions in the emission of CO₂ coupled with these national and global drivers for continued use of fossil fuels necessitates the need for highly efficient and transformational fossil energy systems in the future. Various roadmaps, such as the Coal Utilization Research Council

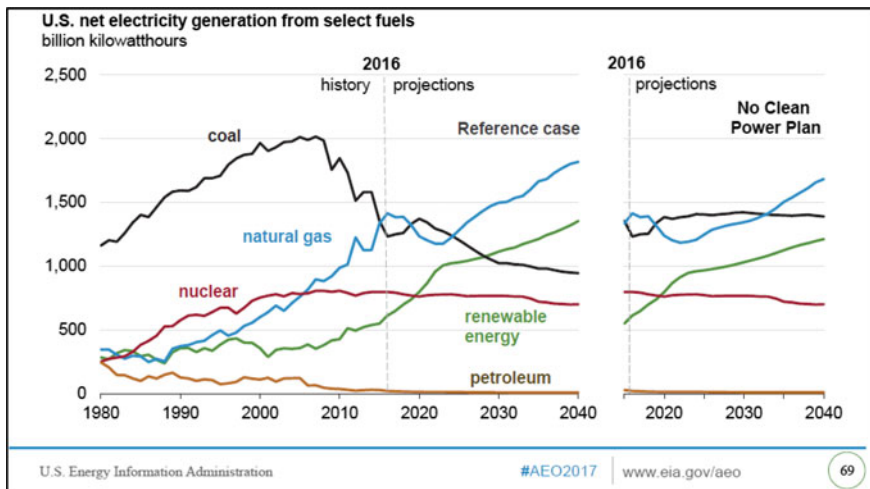


Fig. 1 Historical and projected U.S. electricity generation mix reported by U.S. Energy Information Administration including the reference case scenario (left) and a scenario without adoption of the Clean Power Plan (right) [1]

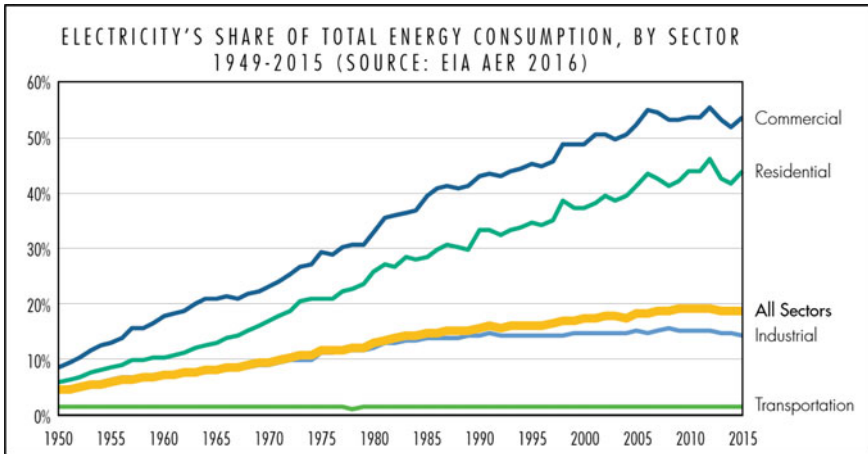


Fig. 2 Historical U.S. electricity use as a percentage of total energy for various sectors showing electricity use has grown faster than total energy for over 50 years [4]

(CURC)-EPRI roadmap [5] and the International Energy Agency (IEA) High Efficiency Low Emission (HELE) roadmap [2, 3] have identified technology pathways first based on maximizing the efficiency of today's technologies and then adopting new transformational technologies. EPRI's Integrated Energy Network (IEN) is a vision for the future in which all energy sources are more efficiently integrated through (a) producing cleaner energy, (b) using cleaning energy through efficiency and electrification, and (c) integrating energy resources [2]. A key aspect of the IEN is the production of cleaner energy through the introduction of new transformational fossil power systems which will lead to cost-effective low carbon fossil generation (likely with carbon capture and storage).

Fossil Power Generation Technologies

Two major technologies identified in the previously mentioned roadmaps are Advanced Ultrasupercritical (A-USC) steam cycles and Supercritical CO₂ (sCO₂) power cycles. These concepts are explored in this paper because, as will be shown, they share many similar structural materials needs and these cycles are required to fully enable future transformational systems, such as an oxygen-fired boiler (oxy-combustion) with carbon capture and an A-USC steam cycle.

Today's pulverized coal-fired (PC) power plants operate at ultrasupercritical (USC) conditions with steam temperatures up to ~610 °C. A-USC conditions generally refer to a steam cycle with steam temperatures of 700 °C and higher. The world-wide development of A-USC technology started initially around 1998 with a variety of European Projects [6]. In 2001, the U.S. Department of Energy in

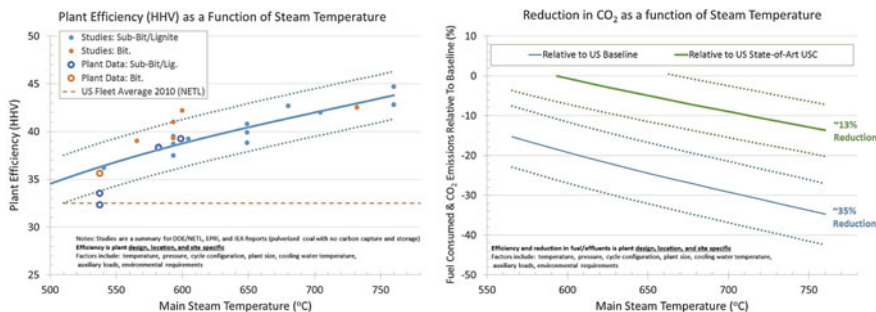


Fig. 3 Effect of steam temperature on pulverized coal-fired powerplant net efficiency (HHV basis) and corresponding reduction in CO₂ [8]

conjunction with the Ohio Coal Development Office (OCDO) and cost share from all the major U.S. boiler and turbine original equipment manufacturers (Alstom, B&W, Foster Wheel, Riley Power, GE, Siemens), the Energy Industries of Ohio (EIO), and the Electric Power Research Institute (EPRI) with support from Oak Ridge National Laboratory (ORNL) and the National Energy Technology Laboratory (NETL) Albany Research Center (ARC) and managed for DOE by NETL, began an ambitious pre-competitive research and development project that would lead to higher efficiency coal-fired power plants with reduced CO₂ emissions [7]. Figure 3 is a summary of pulverized coal-fired plant efficiency (HHV) and emissions reduction, as a function of steam temperature for various U.S. based modeling studies (solid symbols) with some current reported plant efficiency data (open symbols). There is considerable variation due to local conditions (cooling water temperature, fuel type, specific design considerations such as size and utilization of waste heat, etc.). However, when compared to the U.S. Fleet averages of 32.3–32.5% HHV, A-USC conditions are expected to raise efficiency up to 12.5 HHV% which corresponds to a 35% reduction in CO₂ emissions. Even when compared to today’s state-of-the-art USC unit operating at 600 °C (for US Conditions), A-USC offers a CO₂ reduction of ~13%. While an A-USC powerplant has yet to be built, numerous economic studies have shown that in the reduction in operating costs from fuel usage (increase in efficiency) for A-USC does not offset the increased capital cost of the plant, until carbon capture and storage is considered. A-USC becomes economically attractive for carbon reduction, as studies show it is more cost effective to not produce CO₂ in comparison to producing it and then capturing it through carbon capture and storage (CCS). In other regions of the world with more expensive fuel costs or lower labor costs, A-USC may be economically attractive without carbon constraints [9, 10].

Brayton power cycles with supercritical CO₂ (sCO₂) as the working fluid are undergoing intense development for a range of power systems including fossil energy, nuclear power, shipboard propulsion, geothermal energy extraction, and solar thermal power cycles [11]. Principle advantages of the sCO₂ cycle due to the physical properties of CO₂ include compact turbo-machinery, high efficiency, and

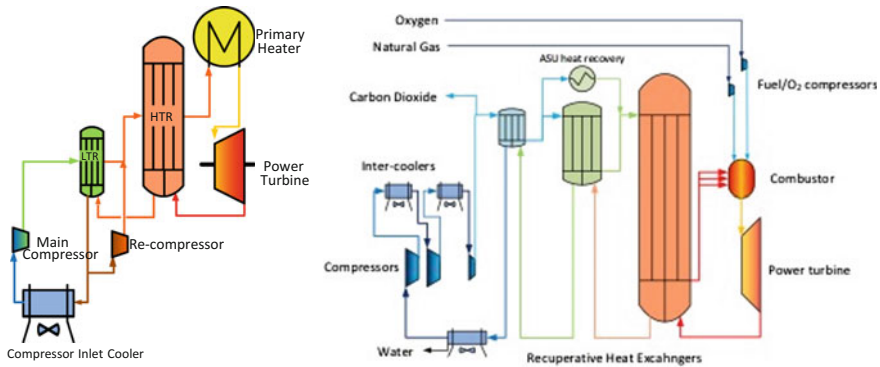


Fig. 4 Examples of general system arrangements for indirect (closed) system (left) and direct (open) cycle (right); note HTR = high temperature recuperator and LTR = low temperature recuperator

the ability to reject heat at higher temperatures when compared to traditional steam Rankine cycles. These advantages may lead to lower capital costs and higher efficiencies for future power systems [12]. Two general types of systems are being investigated as depicted in Fig. 4. Indirect cycles with a closed loop of $s\text{CO}_2$ are being considered for a range of application as the ‘heat-source’ could be coal, natural gas, molten salt, waste heat, etc. To achieve high cycle efficiencies, fluid temperatures of $700\text{ }^\circ\text{C}$ and pressures approaching 300 bar are being considered. Current commercial offerings are only available at smaller sizes $<10\text{ MW}$ and lower temperatures [13]. A more transformational cycle is the direct cycle (right of Fig. 4) which involves direct combustion of natural gas (or gasified coal) and oxygen into a high pressure $s\text{CO}_2$ system. The only byproducts of this approach are high pressure ‘sequestration ready’ CO_2 and water. A pilot plant testing this technology is currently under construction, and to achieve high efficiency the selected fluid temperature is $>700\text{ }^\circ\text{C}$ [13]. Some of the challenges of the $s\text{CO}_2$ system in comparison to a steam Rankine cycle are a narrow heat addition window, the need for extensive recuperation of heat, much higher working fluid recirculation volume, and sensitivity to pressure drop. Many small-scale pilot demonstrations are being investigated to develop these concepts for future power plant applications.

Background on Alloys, Materials Selection, and Completed R&D

Both A-USC and $s\text{CO}_2$ power cycles require materials to withstand high temperatures $> 700\text{ }^\circ\text{C}$ and pressures $> 300\text{ bar}$ for long times. In most cases, the materials for piping, tubing, valves, and heat exchangers are pressure boundary materials and subject to approval to the ASME Boiler and Pressure Vessel (B&PV) Code (or

similar code of construction), while turbine components have more flexibility in selection of materials based on the manufacturers detailed knowledge. At these fluid conditions, the ASME allowable stresses for design are based on the creep-rupture performance of the materials. As stated earlier, major materials development programs in the EU and USA (and later Japan, China, and India) have been working for over a decade to develop the underlying materials technology to make such components available [8]. Figure 5 shows the average 100,000 h rupture strength for various classes of materials. A line at 100 MPa denotes a first cut approximation at the relative temperature capability for materials typically used in today's boilers which shows martensitic/ferritic steels are limited to about 610 °C (highest steam conditions in today's USC power plants). Austenitic stainless steels have higher creep-rupture strength, but poor thermal conductivity and a high coefficient of thermal expansion limit their use to thinner wall components such as tubes due to the generation of thermal stresses in thick components such as boiler headers, turbine casings and discs. Nickel-based alloys are the only alloys available which meet the basic creep-rupture strength requirements for 700 °C+ service. However, there are a range of other properties which are critical for application to A-USC and sCO₂ components including formability, weldability, corrosion resistance, short-term strength, ductility, creep-fatigue performance, weld performance, and manufacturability often in very large section thicknesses. Piping, header, and casing components may require wall thicknesses approaching 100 mm, and there is a need

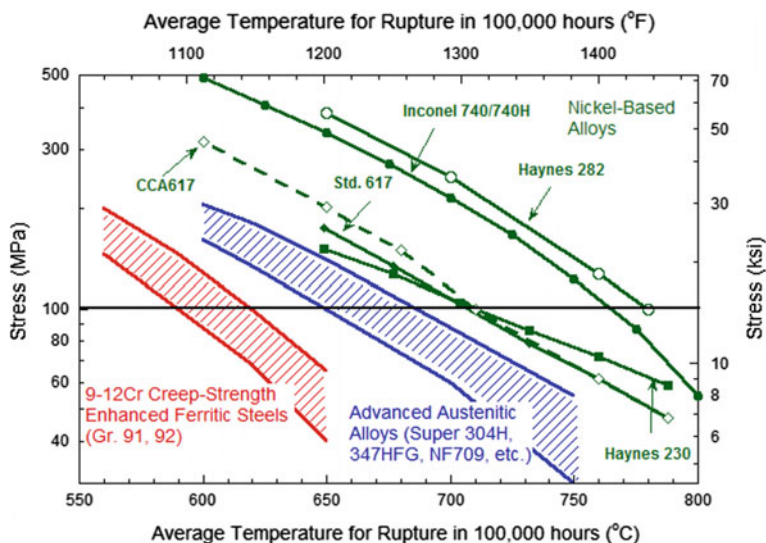


Fig. 5 100,000 average creep-rupture strength for various classes of alloys of interest to A-USC and sCO₂ power cycle application

for large forgings on the order of 1000 mm in thickness for steam turbine rotors. Conventional nickel-based alloys such as Waspalloy and Nimonic 105 which appear to meet the requisite basic creep strength requirements may be used for specific smaller non-welded components such as turbine blades (buckets) and bolting, but these alloys are not code approved nor do they have the weldability and formability for heavy-wall components due to large volume fractions of gamma prime. Similarly, alloys strengthened by gamma double prime such as 718 which have good processing characteristics lose their long-term creep strength above 650 °C, are not code approved, and won't meet creep and tensile strength requirements. Therefore, the main nickel-based alloys of interest to A-USC and sCO₂, shown in Fig. 5 (nominal compositions in Table 1), are either solid solution strengthened with basic temperature capability for approximately 700 °C or gamma prime strengthened with higher capability to about 760 °C. While Table 1 is not an exhaustive list of materials, the material identified have seen the most study predominately by the US and EU for A-USC applications. Currently, the highest-strength code approved alloy is Inconel[®] Alloy 740H[®] which has been successfully welded and fabricated into components up to about 80 mm in thickness. This is a significant technological achievement (along with similar studies and successes on alloys 617, 263, 230, and Haynes 282) in the processing of age-hardenable nickel-based alloys. Table 2 describes some of the research done on various components made with these alloys; more detailed alloy specific information and results from major government led developments is summarized in Ref. [8]. In addition to large section thickness and similar concerns for A-USC steam Rankine systems, sCO₂ Brayton cycles present additional unique nickel-based materials challenges. One challenge is the need for very large pipe diameters due to high recirculation requirements compared to steam; such pipe sizes can only be fabricated through forming and welding. A second consideration is the need to develop processing and performance data for compact heat exchangers with these materials. Compact heat-exchangers are currently made using specialized methods and designs based on combinations of etching, diffusion bonding, brazing, small tubes, fins, and wire meshes which will need to be developed for these nickel-based alloys [14].

A number of recent conferences [11, 22] and summary reports/papers are now available with extensive detail into the laboratory investigations, processing studies, fabrication trials, corrosion performance, and long-term creep behavior of A-USC alloys for boilers [23], turbines [24], and in-plant studies/component demonstration activities [15, 25]. As stated previously, the development of welding procedures for thick sections on age-hardenable materials including forgings, extrusions, and castings represents a significant technological advancement. Figure 6 shows just three examples of the progress made in welding large nickel-based components.

Table 1 Nominal compositions^a of some candidate Ni-based alloys for A-USC and sCO₂ application, wt%

Family	Alloy	ASME code case	C	Ni	Fe	Cr	Mn	Si	Mo	Co	Al	Ti	B	Others
Solid solution	Alloy 617	N06617	0.07	Bal.	0.5	22	0.3	0.3	9	12.5	1.0	0.40		
	CCA617 [*]	N/A	0.06	Bal.	0.3	22	0.1	0.1	9	12	1.2	0.40	0.003	
	Haynes ^b 230	N066230	0.10	Bal.	1.5	22	0.5	0.4	2	0.3	0.3		0.004	W: 14.0 La: 0.02
Gamma-Prime	NIMONIC ^c 263	N/A	0.06	Bal.	0.1	20	0.1	0.1	6	20	0.45	2.2	0.004	
	INCONEL ^c Alloy 740H ^c	2702	0.03	Bal.	1	24.5	0.3	0.15	0.1	20	1.35	1.35	0.001	Nb + Ta: 1.5
	Haynes ^b 282 ^b	N/A ^{**}	0.06	Bal.	0.2	20	0.05	0.1	8.5	10	1.5	2.1	0.005	

^aSulfur and Phosphorous limits omitted from Table^bHaynes, 230 and 282 are registered trademarks of the Haynes International^cINCONEL, NIMONIC and 740H are registered trademarks of the Special Metals Corporation^{*}CCA617 is also designated in literature as 617b or 617 mod^{**}Code Case in Development for Single Age (non-standard) heat-treatment

Table 2 Examples of component production and demonstrations on various A-USC and sCO₂ candidate materials

Material	Component (size or max thickness)	Manufacturing demonstrated	Evaluation method	Notes
CCA617 [15]	Piping system (50 mm)	Pipe and tube production; header component production; piping system fabrication, high-temperature valves	Comtes 700 A-USC Component Test Facility Operation: 20,000 h at 700 °C	Overall good performance and demonstrated many manufacturing and field erection methods, but numerous cracks and failures in thick section components subject to thermal cycles; concluded that all welds needed an additional heat-treatment to avoid stress relaxation cracking
CCA617, 740H [16]	Superheater tubing (10 mm)	Superheater manufacturing including similar and dissimilar metal welding	Steam-Cooled A-USC corrosion test loop: 4 years at 760 °C	Acceptable corrosion performance and no issues identified at welds (note: low operational stress)
740H [17]	Piping (80 mm)	Pipe extrusion and weldability	Destructive laboratory testing	Successful narrow groove welding, validated longer extrusion lengths than same 617 extrusion
740H [18]	Pipes and fittings	Small forgings (hydro-forming, hot forming), thin wall pipe production (rolled formed pipe)	Destructive laboratory testing and Installation in sCO ₂ pilot plant	Pilot plant operation planned for 2018 [19]
263 [8]	Rotor Forging (1000 mm)	Large forging demonstration and rotor welding proof of concept	Destructive testing	Limited data on performance available in literature; some suggestion that alloy optimization for structural stability is still needed

(continued)

Table 2 (continued)

Material	Component (size or max thickness)	Manufacturing demonstrated	Evaluation method	Notes
282 [20]	Rotor Forging (1100 mm disc)	Triple-melt production (2 heats), chemical homogeneity, and disc forging development	Destructive testing	Good processing characteristics suggested larger forging sizes are possible and optimization of grain structure for creep and fatigue were demonstrated
282 [21]	Turbine valve chest (8000 kg pour weight)	Sand casting for turbine cast components (valves and casings)	Destructive testing	First and largest known demonstration of heavy wall 282 casting, size range applicable to steam turbine casings, limited mechanical testing showed acceptable performance

Weldability and Weld Performance

Based on the successful welds made around the globe for A-USC materials, a comprehensive review was conducted by Siefert and colleagues on the fundamentals, weldability, and weld performance of A-USC nickel-based alloys [26, 27]. The major findings and recommendations for the materials listed in Table 1 are highlighted in the following sections, but the reader is encouraged to review references [26, 27] for a more thorough treatment of the subject matter.

Weldability

Nickel-based alloys considered for A-USC and sCO₂ applications may be susceptible to a range of potential weldability issues including: solidification cracking, heat affected zone (HAZ) liquation cracking, ductility dip cracking (DDC), and strain age cracking (SAC) which is also known as stress relaxation cracking. Quantitative ranking of candidate materials for each potential mechanism is problematic because the number of variables which need to be considered include: welding process, shielding gas (if applicable), weld metal composition, base metal composition, grain size, heat-treatment, degree of constraint, sample size/thickness,

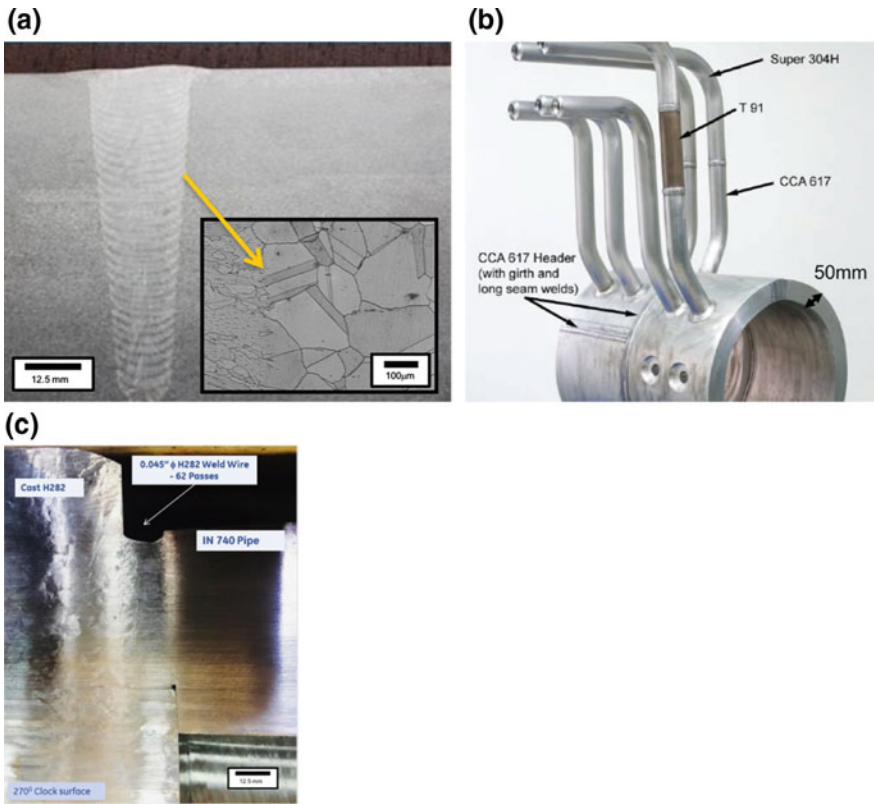


Fig. 6 Examples of successful welding demonstrations on A-USC materials including: **a** cross-sectional micrograph of a 75 mm thick alloy 740H pipe butt weld with no observed welding defects or cracks, **b** multiple orientations and welding processes for a 50 mm thick alloy CCA617 pipe and plate welds on a demonstration header, along with tube dissimilar metal welds, and **c** ~63 mm thick 282 casting to 740H piping weld with 282 filler metal, representing welding to a turbine casing [23, 24]

and welding residual stresses. Furthermore, there exist many non-standardized test methodologies which make comparisons of different studies challenging. However, comprehensive and careful review of the data (when reported) can identify key trends and provide practical mitigation methods if problems are encountered in service.

Fusion Zone Solidification Cracking

Solidification cracking, which occurs in the fusion zone of weldments, is of concern for the candidate alloys. Specifically, many studies have shown that the potential for solidification cracking is sensitive to a host of compositional factors even within the

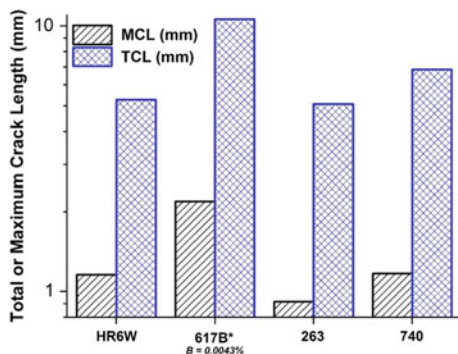


Fig. 7 Trans-varestraint test results for mean and total crack length (MCL and TCL), respectively, gas tungsten arc welding process with 3% loading strain for A-USC alloys after [27, 28]

specification range for the alloys. For alloys 617 and 230, the level of Boron (B) has been found to have a major effect. Figure 7 shows the data gathered for trans-varestraint testing in which a high B heat (0.004 wt%) of 617 exhibited a higher tendency to solidification cracking (as measured by crack length) compared to alloys 263 and 740. HR6 W, a laves phase strengthened Ni-Fe-Cr alloy with 6–8 wt%W and candidate A-USC temperatures <700 °C was included in this study as well. Figure 8 shows results for testing on Haynes 230 where B free heats exhibited fewer cracks compared to heats with 0.004–0.006 wt% B. In general B is added to improve high-temperature creep behavior and microstructural stability in nickel-based alloys, but care must be taken to ensure weldability challenges are minimized. In the case of Haynes 230 for example, matching filler metals are essentially free from B to reduce concerns over solidification cracking.

Liquation Cracking

Nickel-based alloys typically exhibit a wide melting and solidification range depending on alloying additions. In general, the wider the solidification range combined with specific alloying elements can lead to HAZ cracking in areas of the base metal near welds which may undergo partial melting during welding cycles. Liquation cracking was first identified in alloy 740 during microstructural examinations of thick section welding trials including base metal HAZ cracking as well as weld metal cracking. Figure 9 shows the ‘Nil Ductility Range’ (NDR) for a host of 740 and modified 740 compositions along with other nickel-based alloys [30]. Based on these results and other similar studies including computational thermodynamics to help understand how alloying elements segregated and created low-melting point locations in the material, an optimized 740H composition with reduced B, Si, and Nb was produced. Multiple welding trials (see Fig. 6) have shown this composition to be resistant to liquation cracking. Figure 9 also shows

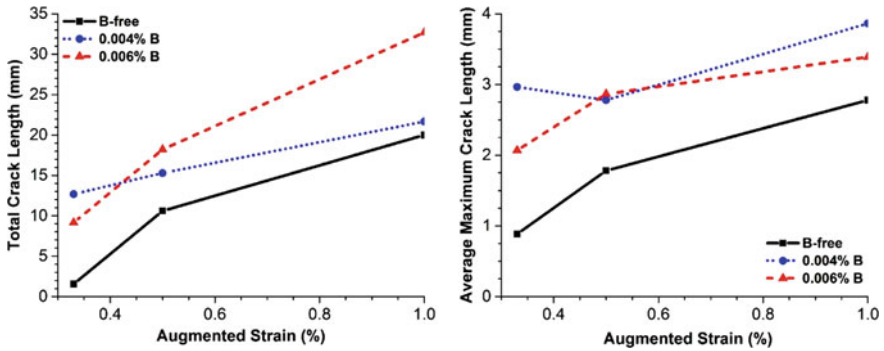


Fig. 8 Influence of Boron on alloy 230 hot cracking tendency as measured by varestraint testing [27, 29]

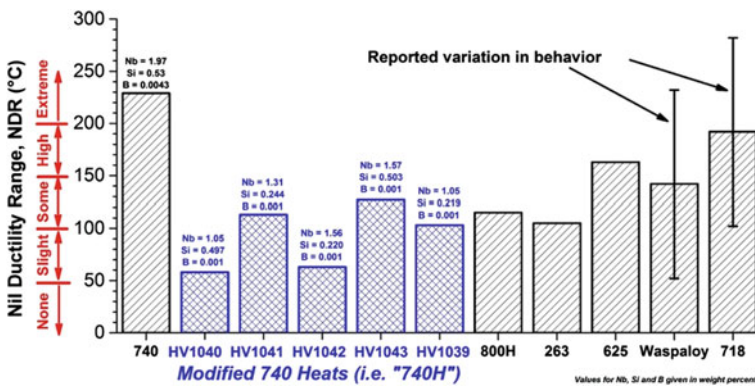


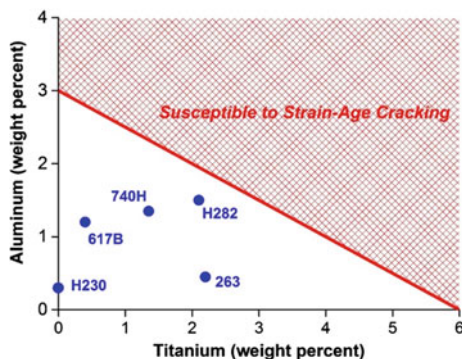
Fig. 9 Comparison of NDR for various heats of alloy 740 compared to other A-USC and nickel-based alloys. Alloy modifications to optimize the 740 composition within the compositional range, now known as 740H, show significant reduction in tendency to form liquation cracks [27, 30]

data for other common nickel-based alloys including alloy 625, Waspaloy, and 718. This comparison shows that the individual heat trials on the modified 740H should perform as good or better than these commonly used alloys. It should be noted that while 718 is generally considered a fabricable and weldable alloy due to slow precipitation kinetics, a number of studies have shown it can, in some cases, be susceptible to liquation cracking [31, 32]. Thus in Fig. 9, a range of behavior from ‘slight’ to ‘extreme’ is reported. For 718 grain size, cast versus wrought structure, and compositional factors (Mn, Si, etc.) have been shown to be critical to the susceptibility of the alloy to this cracking mechanism [32].

Strain Age and Stress Relaxation Cracking

Strain age cracking (SAC) and stress relaxation cracking are often interchanged, but generally SAC refers to cracking which occurs during post weld heat-treatment or high-temperature service. The fundamental basis for SAC is that rapid precipitation in the alloys during high-temperature exposure (PWHT or service) causes an increase in strength and decrease in material ductility. If this change happens before residual stresses from welding are able to relax (from the high temperature exposure during PWHT or service), the material may crack to relieve the stresses. Thus, it is a very complex mechanism which depends on level of residual stress, precipitation kinetics, and material behavior all of which are affected by time, temperature, composition, and component plus weld geometry. SAC is one reason many nickel-based alloys are considered ‘unweldable’ or have very poor or limited weldability in only thin sections (low residual stresses). Classically, this susceptibility is measured by the amount (volume fraction) and rate of gamma prime precipitation which is related to the amount of Al and Ti as shown in Fig. 10. This figure helps show why for A-USC and sCO₂ applications, the alloy being investigated have <25% gamma prime. In practice, this figure does not take into account the kinetics of gamma prime and other hardening addition formation (such as carbides), changes in ductility with time and aging, nor does it address other alloying elements such as Nb which contributes to gamma prime and gamma double prime strengthening. The simplicity of Fig. 10 is misleading. Many laboratory studies have reached different conclusions on the ranking and susceptibility of A-USC alloys to SAC. In some cases, the age hardenable alloys appeared worse than the solid solution alloys, but in other cases the reverse was observed. In practical application, SAC (relaxation cracking) was reported to be widespread in alloy 617 components in the EU Comtes700 [15]. Studies on 617 show that PWHT, pre-strain/stress, composition, grain size, and the specific temperatures of application will radically change the alloy’s susceptibility to this failure mechanism. Such studies and an industry agreed upon testing approach has not been established for the other alloys under consideration but, some work is currently ongoing to develop a more global approach to the problem [33].

Fig. 10 Location of typical A-USC alloys on a Strain-Age Cracking susceptibility diagram. Note, this diagram is based on potential to form gamma prime precipitates; in practice, other precipitates such as carbides may also affect SAC



Summary on Weldability

Most of the published weldability studies and the susceptibility to cracking on A-USC nickel-based alloys focus on alloy 617 and 740H. Clear conclusions from this research have shown the practical importance of specifying the 740H composition to reduce the tendency for liquation cracking and the need for many 617 components to be given a PWHT to combat SAC. For alloys such as 230, 263, and 282, there is need for additional studies to vet the alloys performance for solidification cracking, liquation cracking (both HAZ and weld metal), and SAC. In general, all candidate materials are inherently susceptible to solidification cracking and liquation cracking. SAC or relaxation cracking is also a concern, but the complexity of the problem, lack of understanding of residual stresses, and lack of a standardized test method provides a challenge to the research community to further the science, perhaps through a combination of available computational methods to address fundamental material chemistry and precipitation kinetics, experimentation to validate models, and field testing to confirm. Finally, there is virtually no data on these alloys in the cast state. Alloy 282 is considered a key candidate for turbine casing and valve body castings, but no weldability studies (beyond very limited demonstration articles) have been conducted to assess how chemical inhomogeneity and large grain size/dendritic spacing effects weldability.

Weld Performance

High-temperature creep performance (strength and ductility) is a critical criterion for these future transformational power systems, and experience has shown that welds are often the 'weakest link' in the system. To that end, weldability (the ability to make a sound weld without cracking and exhibiting room temperature tensile properties nearly equivalent to the base metal) must also consider weld performance for these alloys. Based on the comprehensive review of the available creep-rupture data on weldments and weld metal for 617, 230, 263, 740/740H, and 282 [27], major deficiencies in data, reporting, and understanding were identified. Only 617 (and variants) and 740H have appreciable reported cross-weld creep-rupture databases (over 80 data points for each alloy were gathered), but even for these alloys basic information such as specimen size, welding details, PWHT and failure location are inconsistently reported (if reported at all). To plot disparate datasets, the Larson Miller Parameter (LMP) using a universal constant of 20 was used to show general trends in the data in comparison to base metal behavior. Figure 11 is a plot of the 617 data for matching filler metals segmented by welding process. What is clear is a vast scatter depending in part on the welding process. For CCA617, non-flux welding processes (GTAW for example) generally show improved creep life over fluxed (SMAW and SAW) processes. It should also be noted that a few of the data points extend to >30,000 h but many are short-term tests of <1,000 h. Limited studies (optical microscopy) have been conducted on some samples [27],

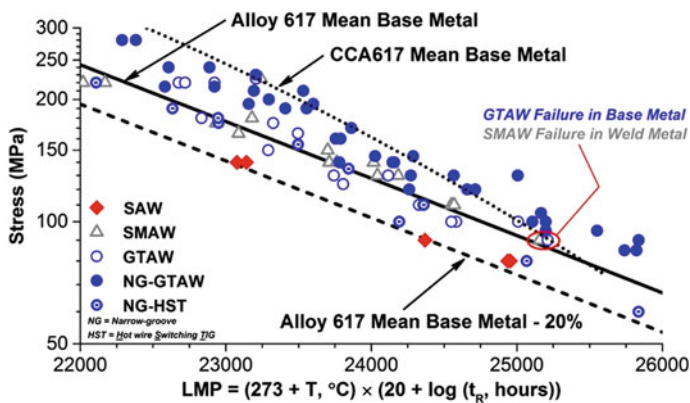


Fig. 11 Compilation of cross-weld creep-rupture data on alloy 617 and CCA617 segmented by welding process and plotted using a Larson Miller Parameter (LMP, $C = 20$) for welds with nominally matching 617-type filler metals [27]

but even with the long-term test data, there is an extreme lack of detailed metallurgical work on the weldments to understand the underlying metallurgical factors effecting weld performance.

Codes and standards often use weld strength reduction factors (WSRFs) as a convenient way to represent the behavior of welds. There is not standardized approach to the calculation or application of WSRFs (which also does not account for sample size and the complexity of creep-failure mechanisms). Never-the-less, various WSRFs for 617 have been reported from the available data which generally show WSRFs of 0.8–1.0 (meaning 80–100% of the base metal strength) in cross-weld creep. The use of an alloy 617 WSRF is complicated by the choice of baseline non-welded data, which are the solid and dotted lines in Fig. 11, where most data points for GTAW welds are observed failing above the average 617 baseline but below the modified CCA617 average strength; the choice of 617 or CCA617 baseline effects the calculation and application of a WSRF.

Alloy 740/740H rupture data are plotted in Fig. 12 for matching and non-matching consumable welds (no autogenous welds have been evaluated in creep). Limited rupture times beyond 10,000 h are included in this dataset, but most of the data are for relatively short times. For 740H, the matching filler metals in the welded and aged condition do not perform as well (generally) in comparison to alternative filler metal 282 and 263. Only one detailed microstructural study has been undertaken to understand how the formation of precipitate coarsened zones in 740H weld metal lead to degradation in creep resistance of the weldment (failure locations was in the weld metal) [34], and the improvement in behavior using 282 and 263 filler metals has not been studied in detail. Additionally, only 740H welds with weld metal failures have been investigated so the mechanism of failure for cross-weld HAZ failures is unknown at this time. Furthermore, solution annealing appears to improve the performance of the 740H weld metal, but for the limited

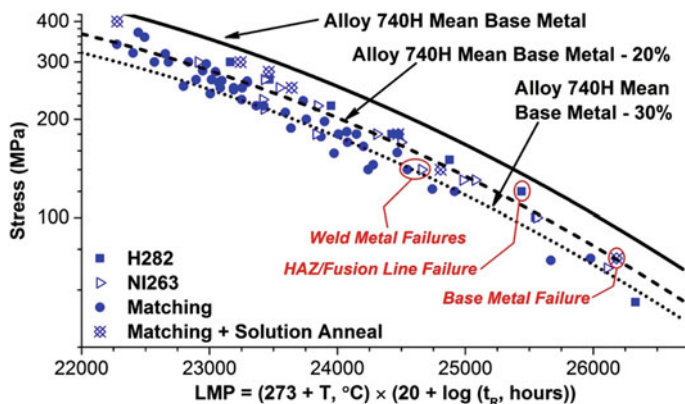


Fig. 12 Compendium of 740/740H cross-weld creep-rupture data for welds made with matching filler metals (multiple processes) compared to alternative filler metals (282 and 263) and solution annealed matching filler metal welds [27]

dataset investigated did not fully restore the creep strength to base metal levels. For WSRFs, the ASME B&PV code case (CC2702) uses a conservative 0.7 factor for application to seam welds due in part to the uncertainty surrounding the data (this is plotted as mean—30% in Fig. 12).

Much more limited creep-rupture datasets are available on alloys 230, 282, and 263. In general, alloy 230 shows some reduction (WSRF of 0.8) due, speculatively, to the elimination of B in the weld metal. The data show better performance for 282 and 263, but most are short-term creep without supporting failure information (ductility and failure location). Thus, there is a large data gap for application of these alloys. It should be noted that such WSRF values for all the nickel-based alloys (0.7–1.0) are similar to values reported and utilized in USC powerplant steels, such as Grade 91 and 92.

In conclusion, there is a scarcity of weld performance data for many of the alloys being considered for A-USC and sCO₂ application. Furthermore, new joining methods for small channel heat-exchangers such as brazing and diffusion bonding, have not been evaluated for performance at high temperature conditions. In cases where data do exist, critical information including weld metal chemistry, failure location, and ductility are rarely reported, making the development of WSRFs problematic. Surprisingly there is an extreme lack of detailed microstructural characterization despite the fact that metallurgically complex weldments are locations where long-term damage often initiates. One final note is that in the future, power plant cycling is expected. No work (in the public domain) to the authors knowledge has been done to look at weld cyclic behavior (fatigue and creep-fatigue) to compliment the cyclic data on the base metals.

Summary and Conclusions

Nickel-based alloys including age-hardenable materials such as 263, 740H, and 282 are critical to enabling the next generation of transformational fossil power systems incorporating A-USC steam Rankine cycles and sCO₂ Brayton cycles. A large body of fundamental materials R&D has been completed including significant laboratory research and shop fabrication studies. Limited field testing supports continued evaluations through ongoing work in pilot scale testing. Major strides have been made to fabricate and weld these materials, but a critical review of weldability and weld performance shows much more research is needed to fully understand weldability, weld performance, and weldment microstructural evolution to help define design limits to ensure successful component durability.

References

1. U.S. Energy information administration. Annual energy outlook. #AEO2017. www.eia.gov/aeo. Accessed 5 Jan 2017
2. Diczfalusy B (2012) HELE coal technology roadmap. In: IEA clean coal centre workshop: on advanced ultrasupercritical coal-fired power plants, Sept 2012, Vienna, Austria, pp 12–20
3. Burnard K, Ito O (2012) HELE coal technology roadmap. In: IEA clean coal centre workshop on advanced ultrasupercritical coal-fired power plants, Sept 2012, Vienna, Austria, pp 12–20
4. The integrated energy network: connecting customers to reliable, safe, affordable, and cleaner energy. EPRI, Palo Alto, CA, EPRI Report Number 3002009917 (2017). www.epri.com
5. The CURC-EPRI coal technology roadmap July 2015. www.coal.org
6. Blum R, Vanstone R (2003) Materials development for boilers and steam turbines operating at 700 °C. In: Proceedings to the 6th international Charles Parsons materials conference. Dublin, Ireland
7. U.S. department of energy and Ohio coal development office advanced ultra-supercritical materials project for boiler and steam turbines. EPRI, Palo Alto, CA, Mar 2011. EPRI Report Number 1022770. http://my.epri.com/portal/server.pt?Abstract_id=00000000001022770
8. Materials for ultra-supercritical and advanced ultra-supercritical power plants ©2017, Elsevier Ltd., UK, p 692. ISBN 978-08-100552-1
9. Engineering and economic evaluation of 1300F series ultra-supercritical pulverized coal power plants: phase 1. Palo Alto, CA, EPRI Report Number 1015699 (2008)
10. Cost and performance baseline for fossil energy plants—volume 1: bituminous coal and natural gas to electricity. DOE/NETL-2010/1397. www.netl.doe.gov
11. Proceedings to the 6th International symposium on supercritical CO₂ power cycles. 27–29 Mar 2018, Pittsburgh, PA. <http://sco2symposium.com/www2/sco2/>
12. Fundamentals and applications of supercritical carbon dioxide (sCO₂) based power cycles. Woodhead Publishing. ©2017 Elsevier Ltd. ISBN 978-0-08-100804-1
13. Novel cycles database report 2017. Palo Alto, CA, EPRI Report Number 3002012116 (2017)
14. Wright IG, Pint BA, Shingledecker JP, Thimsen D (2013) Materials considerations for supercritical CO₂ turbine cycles. In: Proceedings of ASME turbo Expo 2013: turbine technical conference and exposition. GT 2013, 3–7 June 2013, San Antonio, TX, USA. GT2013-94941 ©ASME
15. Component test facility for a 700C power plant (Comtes700) EUR 25921EN ©European Union (2013). ISBN 978-92-79-29379-5. <https://doi.org/10.2777/98172>

16. Bordenet B et al (2015) Steam oxidation and fireside corrosion testing of several advanced alloys in a steam loop at A-USC design temperatures. In: Proceedings of EPRI international conference on corrosion in power plants. EPRI, Palo Alto, CA, EPRI Report Number 3002006972
17. Baker BA, Gollihue RD (2011) Proceedings to the 6th international conference on advances in materials technology for fossil power plants, Santa Fe, New Mexico, 30 Aug–4 Sept, 2010. Mar 2011, EPRI 1022300. Distributed by ASM International, pp 96–109
18. deBarbadillo JJ, Baker BA, McCoy SA (2016) Alloy 740H—development of fittings capability for A-USC applications. In: Proceedings from the eighth international conference on advances in materials technology for fossil power plants, Oct 11–14, 2016. Albufeira, Algarve, Portugal. Published by ASM International ©2016, EPRI Report Number 3002008446
19. Christopher J (2017) Natural gas plant makes a play for coal’s market, using ‘clean’ technology NPR. <https://www.npr.org/2017/04/07/522662776/natural-gas-plant-makes-a-play-for-coals-market-using-clean-technology>. Accessed 10 Apr 2017
20. Saha D et al (2016) Qualification of UNS N07028 for forged steam turbine rotors. In: Proceedings from the eighth international conference on advances in materials technology for fossil power plant, Oct 11–14, 2016. Albufeira, Algarve, Portugal. Published by ASM International ©2016, EPRI Report Number 3002008446
21. Thangirala S, Myers J (2016) Development of large sand castings of Haynes 282 for A-USC turbines. In: Proceedings from the eighth international conference on advances in materials technology for fossil power plants, Oct 11–14, 2016. Albufeira, Algarve, Portugal. Published by ASM International ©2016, EPRI Report Number 3002008446
22. Parker J, Shingledecker J, Siefert J (2016) Advances in materials technology for fossil power plants. In: Proceedings from the eighth international conference on Oct 11–14, 2016. Albufeira, Algarve, Portugal. Published by ASM International ©2016, EPRI Report Number 3002008446
23. Purgert R, Shingledecker J, Pschirer J, Ganta R, Weitzel P, Sarver J, Tortorelli P (2015) Boiler materials for ultra supercritical coal power plants. United States. <https://doi.org/10.2172/1346714>
24. Purgert R, Shingledecker J, Saha D, Thangirala M, Booras G, Powers J, Hendrix H (2015) Materials for advanced ultrasupercritical steam turbines. United States. <https://doi.org/10.2172/1243058>
25. Purgert R, Phillips J, Hendrix H, Shingledecker J, Tanzosh J (2016) Materials for advanced ultra-supercritical (A-USC) steam turbines—A-USC component demonstration, United States. <https://doi.org/10.2172/1332274>
26. David SA, Siefert JA, Dupont JN, Shingledecker JP (2015) Weldability and weld performance of candidate nickel base superalloys for advanced ultrasupercritical fossil power plants part I: fundamentals. *Sci Technol Weld Join* 20(7):532–552
27. Siefert JA, Shingledecker JP, Dupont JN, David SA (2015) Weldability and weld performance of candidate nickel base superalloys for advanced ultrasupercritical fossil power plants part II: weldability and cross-weld creep performance. *Sci Technol Weld Join* <http://dx.doi.org/10.1179/1362171815Y.0000000094>. Accessed Oct 2015
28. Saito N, Komai N, Takei Y (2014) Fabrication trials of Ni-based alloys for advanced USC boiler application. In: Proceedings from the seventh international conference on advances in materials technology for fossil power plants. ASM International, pp 190–201
29. Ernst SC (1994) Weldability studies of Haynes 230 alloy. *Weld J* 73(4):80–89
30. Ramirez JE (2012) Susceptibility of IN740 to HAZ liquation cracking and ductility dip cracking. *Weld J* 91(4):122–131
31. *Welding metallurgy and weldability of nickel-base alloys*. Wiley, Hoboken, New Jersey, USA (2009)
32. Lucas MJ et al (1970) The welded heat-affected zone in nickel base alloy 718. *Weld Res Suppl* 45–54

33. Kant R, DuPont J (2017) Stress relaxation cracking susceptibility of high temperature alloys. In: Presentation of 12th international conference on EPRI welding and repair technology for power plants June 20, 2017. Kissimmee, FL, USA
34. Bechetti DH, DuPont JN, Siefert JA, Shingledecker JP (2016) Microstructural evolution and creep-rupture behavior of A-USC alloy fusion welds. *Metallurg Mater Trans A* 1–17. <https://doi.org/10.1007/s11661-016-3603-7> Accessed June 2016